

Nernst-Ettingshausen coefficient measurements on Al below 1 K

A. Amjadi* and J. Bass

Department of Physics and Astronomy, Michigan State University, East Lansing, Michigan 48824

(Received 7 May 1987)

A system has been constructed for high-sensitivity transport measurements with a dilution refrigerator in magnetic fields up to 3 T and used to measure the high-field Nernst-Ettingshausen coefficient of Al below 1 K. For magnetic fields up to 2 T, the data are consistent with a simple electron-phonon mass-enhancement factor of $1+\lambda$. Data above 2 T were not sufficiently reliable to analyze.

I. INTRODUCTION

There now exists a consensus among theorists that thermoelectric coefficients display many-body enhancements, such as the electron-phonon mass-enhancement factor¹⁻³ λ , and that the high-magnetic-field Nernst-Ettingshausen (NE) coefficient should be enhanced simply by $1+\lambda$.^{3,4} Experimental data on Al (Refs. 1 and 5) and Mo (Ref. 6) are consistent with this expectation, but extend down only to about 1.5 K where phonon-drag contributions remain significant. To eliminate uncertainties due to phonon-drag, and because of the small possibility that measurements to much lower temperatures might show deviations from predicted behavior, we decided to extend NE measurements on Al to well below 1 K. This paper reports the results obtained. It is organized as follows. Section II briefly describes what we measure and how we isolate the mass enhancement. Section III contains a discussion of experimental techniques and procedures, further details of which are given elsewhere.⁷ Section IV contains our experimental data and analysis. Section V contains a summary and conclusions.

II. QUANTITIES TO MEASURE

Using the notation of Douglas and Fletcher,⁸ the transport equations relating the electrical and thermal current densities \mathbf{J} and \mathbf{U} to the electric field \mathbf{E} and the temperature gradient ∇T , are

$$\mathbf{J} = \vec{\sigma} \cdot \mathbf{E} - \vec{\epsilon}'' \cdot \nabla T, \tag{1a}$$

$$\mathbf{U} = -\vec{\pi} \cdot \mathbf{E} - \vec{\lambda}'' \cdot \nabla T. \tag{1b}$$

Here $\vec{\sigma}$, $\vec{\epsilon}''$, $\vec{\pi}$, and $\vec{\lambda}''$ are, respectively, the electrical conductivity, the thermoelectric, the Peltier, and the thermal conductivity tensors, all of which are functions of the magnetic field \mathbf{B} and the temperature T .

For an uncompensated metal like Al, and \mathbf{B} directed along the z axis, the quantity of interest is the adiabatic NE coefficient⁵

$$P^a = E_y / U_x = \frac{V_y / W}{Q_x / Wt} = \frac{V_y t}{Q_x} \tag{2}$$

with the boundary conditions $\mathbf{J} = \mathbf{0}$ and $U_y = 0 = U_z$. In Eq. (2), W is the sample width, t the sample thickness, V_y the transverse voltage across the width of the sample, and Q_x the total heat current passing through the center of the sample. We see from Eq. (2) that to determine P^a , we must measure V_y , Q_x , and t .

In the high-magnetic-field limit, the diffusion component of P^a , say P_d^a , is given by⁵

$$P_d^a = (\epsilon''_{xy} \rho_{yx}) / \lambda''_{xy} = -\gamma' B / [L_0 (n_e - n_h)^2 e^2]. \tag{3}$$

Here B is the magnitude of the magnetic field, L_0 is the Sommerfeld Lorenz number $2.443 \times 10^{-8} \text{ V}^2/\text{K}^2$, e is the electronic charge, n_e and n_h are, respectively, the number of electrons and holes per unit volume in the metal, and $\gamma' = \pi^2 k_B^2 N(\mu) / 3$, where k_B is Boltzmann's constant and $N(\mu)$ is the electronic density of states at the Fermi energy μ . γ' has exactly the same form as the electronic specific heat, $\gamma^c = \pi^2 k_B^2 N(\mu) / 3$, where we have used the symbols γ' and γ^c to designate the "transport" and "specific heat" coefficients, respectively, so as to make a distinction which can be tested experimentally. γ^c is known, on very general grounds,⁹ to contain an electron phonon enhancement of just $1+\lambda$. Our experimental task is thus to measure the ratio γ' / γ^c and see whether it is equal to unity. If it is, then the NE coefficient is enhanced simply by $1+\lambda$.

III. EXPERIMENTAL TECHNIQUES AND PROCEDURES

For a constant temperature difference and fixed magnetic field, the NE voltage V_y decreases linearly with decreasing temperature, and is thus more difficult to measure at lower sample temperatures. Moreover, at lower temperatures, smaller temperature differences are needed to keep the average sample temperature low. V_y can be increased by increasing B , but the application of too large a magnetic field to Al will lead to magnetic breakdown.¹⁰ NE measurements below 1 K on Al thus require very sensitive voltage measurements in the presence of a relatively large magnetic field (~ 2 T). For a sample thickness of 0.05 mm, and a temperature difference of 0.04 K along the sample length of 2 cm, the NE coefficient of Al is expected to produce a voltage of

about 10^{-10} V at 0.2 K in a field of 2 T. To measure this voltage with an accuracy approaching 1% thus requires a voltage sensitivity of 10^{-12} V, which can easily be obtained with a superconducting quantum interference device (SQUID).¹¹ However, SQUID's are extremely sensitive to magnetic flux, so that extreme care in vibration isolation of the sample, and its current and potential leads, is essential if vibration in the 2-T field is not to produce noise voltages much greater than 10^{-12} V when the sample is mounted on the mixing chamber of a dilution refrigerator. To make the measurements described in this note we had to construct a unique system. This system is described below, with further details given elsewhere.⁷ With this system we were able to reduce voltage noise to about 10^{-13} V in the presence of a magnetic field of 3 T for a sample cooled to 0.1 K. We were also able to measure temperatures to a fraction of a percent and temperature differences with the accuracy of several percent needed for quantitative NE coefficient measurements.

A. Dilution refrigerator

The sample was cooled using a locally built dilution refrigerator,¹² with a cooling capacity of $\sim 150 \mu\text{W}$ at 0.15 K and $\sim 40 \mu\text{W}$ at 0.1 K. This capacity limited the heat which could be put into the sample, and thus the temperature gradient used to produce the NE effect.

B. The magnet, magnet support, and vibration isolation

The magnet used in these measurements was an Oxford Instruments, model K1034, 5-T superconducting solenoid, with an inner diameter of 5 cm. The field was homogeneous in the z direction to 0.1% over the center 2.5 cm. A superconducting switch, in parallel with the magnet, allowed the magnet to be operated in persistent current mode with the power supply disconnected. To minimize He boil off due to a combination of thermal conduction and Joule heating in the wires carrying current to the solenoid, the thick wires carrying current at room temperature were wrapped around a cylindrical Cu heat sink in the He gas at the top of the cryostat, and then connected to a parallel combination of thinner Cu wires and superconducting wires which went down to the magnet.

Because of the sensitivity of SQUID's to an applied magnetic field, the sample could not be allowed to vibrate relative to the superconducting magnet used to apply the field. Vibration isolation and rigid contacts were thus essential problems of experimental design. The dilution refrigerator was isolated against external vibration using a Newport Research, air-mount, vibration isolation stand, topped with a wooden structure filled with sand.¹² The pumping lines were brought to the refrigerator through flexible double bellows. The system for attaching the sample and the superconducting magnet rigidly to the mixing chamber of the refrigerator, while maintaining thermal isolation except where thermal contact was desired, is shown in Fig. 1.

The magnet (*G*) was attached to the flange at the top of the vacuum can by three long, 0.64-cm-diam, thread-

ed brass rods (*B*), located inside the helium bath. Brass was chosen so that when the system cooled, the brass would contract more than the stainless-steel upper portion of the vacuum can and cause the magnet to push upward on the can, thereby keeping its connections leak tight. The magnet was attached to the body of the vacuum can by two Teflon rings (*C* and *H*), which at room temperature provided a slight clearance between the magnet and the can, but shrank upon cooling so that the magnet and the can were rigidly connected.

The mixing chamber was connected to the vacuum can using a "reentrant-spider"¹³ centering device (*A*), described elsewhere.⁷ This device provided rigid

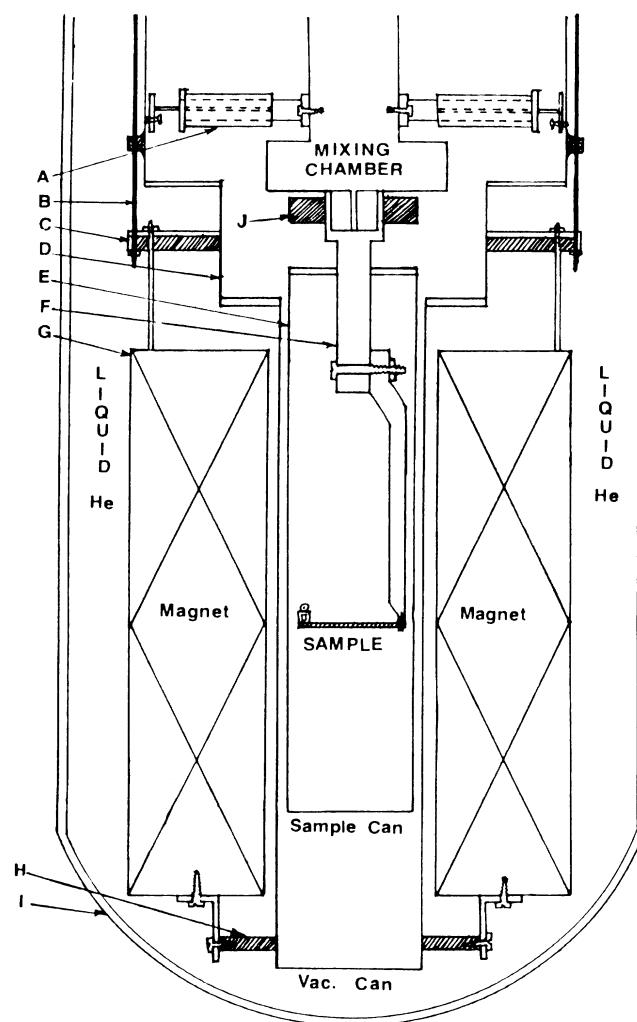


FIG. 1. The assembled system, consisting of the sample in the sample holder, the centering device, and the superconducting magnet. The entire system is inside a liquid-helium double Dewar. The letters designate the following items. *A*, centering device; *B*, magnet support; *C* and *H*, Teflon rings for rigidly connecting the magnet to the vacuum can; *D*, vacuum can; *E*, sample can; *F*, sample support; *G*, magnet; *I*, liquid-helium Dewar; *J*, Teflon ring for clamping the sample holder to the mixing chamber.

mechanical contact between the mixing chamber and the vacuum can, while maintaining a two-stage thermal isolation of the mixing chamber from the 4.2-K bath surrounding the can. The sample can could be centered using screws on the outside of the centering device that could be adjusted from underneath, after removal of the bottom half of the vacuum can. To permit this access, the vacuum can was made out of two parts which attached together just beneath the centering device.

C. The sample

The sample material was 99.999% pure Al [initial bulk residual resistance ratio (RRR) equal to $R(300\text{ K})/R(4.2\text{ K}) = 20\,000$] which had been purified and then rolled into a foil of thickness 0.05 mm by Cominco Inc. The length (2.6 cm) and width (0.32 cm) of the sample were limited by the 5-cm inner diameter of the superconducting magnet. The sample was shaped (Fig. 2) with a spark cutter to have six symmetrically placed limb extensions for attaching potential leads and thermometers, and two wider ends for thermal and electrical current inputs. After spark cutting, the sample was placed between two very clean pieces of alumina to keep it flat, annealed at 420°C for 12 h, and then slowly cooled in 5 h. After annealing, the sample was glued to a thin Vespel substrate for attaching to the sample holder. The RRR of the annealed sample was 2300.

D. The sample holder

As shown in Fig. 2, the sample rested on a Vespel substrate. Brass screws were used to screw the sample and the substrate into a rigid copper support. This support, in turn, was screwed into a second rigid copper support (*F* in Fig. 1) on the mixing chamber of the dilution refrigerator. To improve thermal contact by eliminating oxide formation, the contact surfaces between the sample and the first copper support, and between the first support and the second one, were gold plated. To further improve the thermal contact between the sample and the mixing chamber, the ends of a separate wire of pure, polycrystalline Ag were spot welded to the cold end of the sample and to the mixing chamber, respectively.

E. Electrical contacts

Three pairs of 0.01-mm-diam superconducting NbTi potential leads were attached to the sample: one pair for sending electrical current into the sample, and two pairs for measuring longitudinal and transverse voltages, respectively, across the sample. The best procedure for achieving low resistance, stable contacts of the NbTi to the sample was found to be a combination of plating and solder as described elsewhere.⁷ To minimize pickup noise from the magnetic field, each pair of wires was twisted carefully together, starting from as close to the sample as possible, and fed out from the sample through a Pb tube.

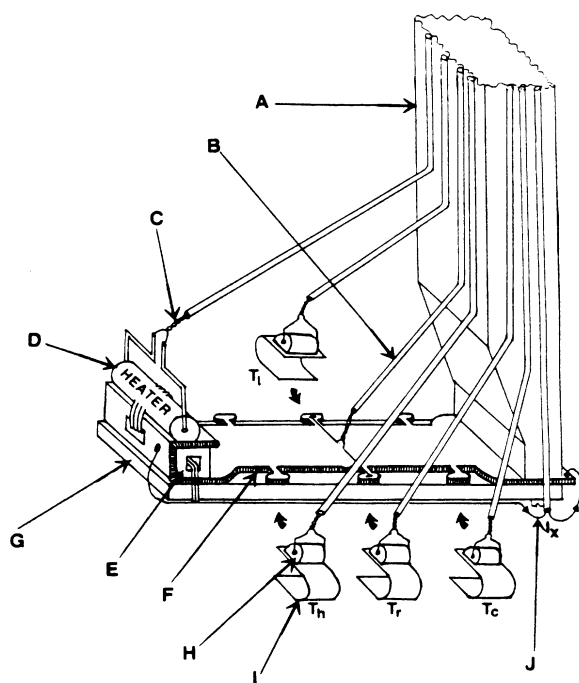


FIG. 2. The sample in the sample holder. The letters designate the following items. *A*, main Cu support; *B*, Pb shield around twisted potential leads; *C*, twisted heater leads; *D*, heater; *E*, heater stand; *F*, Al sample; *G*, Vespel substrate; *H*, thermometer; *I*, thermometer spring-clamp; *J*, current leads to the sample. The symbols T_h , T_c , T_l , and T_r designate the "hot," "cold," "left," and "right" thermometers, respectively.

F. The heater, temperature measurement, and temperature control

The heater used to produce a temperature gradient across the sample was a wire-wound resistor that was attached to the sample using cigarette paper saturated with General Electric No. 7031 varnish, as shown in Fig. 2. The resistor was heated with a dc current, which was measured by passing it through a known resistance in series with the heater, and measuring the voltage across this resistance using a digital voltmeter. The heat input could be determined with an accuracy of about 0.1%.

Temperatures across the sample were measured using small 100- Ω , $\frac{1}{4}$ -W Speer carbon resistors, which were first cut into disks about 3 mm long and then sanded flat on one side (Fig. 3) so that they could be rigidly attached to flat nonmagnetic springs (Fig. 2) that clamped onto elliptical pads on the sample. The flattened side of the thermometer was electrically isolated from the spring by means of cigarette paper saturated with GE No. 7031 varnish. The interface between the spring and the pad was coated with Apiezon N-Grease to ensure good thermal contact. The thermometer leads were 0.01-mm-diam NbTi leads, which were attached to the sides of the resistor with silver paint. When the paint was dry, the thermometers were baked at 200°C for 10 h to

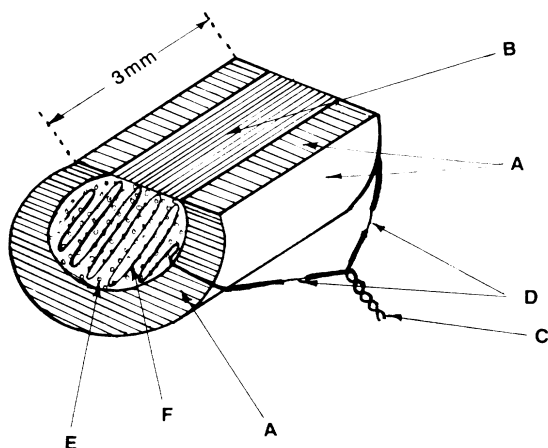


FIG. 3. Speer carbon resistor prepared as a thermometer. A, resistor outer body; B, exposed and flattened graphite core; C, twisted superconducting NbTi leads; D, Cu cladding removed from the superconducting wire; E, silver paint for electrical contact between the leads and the graphite core; F, superconducting NbTi with the electrical insulation removed.

fully establish the silver-to-resistor contact. The thermometers were then painted with Duco cement, and a little silicon glue was placed on the leads at the ends of the thermometer to provide strength with flexibility. This procedure was found to yield robust thermometers with calibrations that did not change significantly from run to run. The leads were twisted together to minimize any loops, and the copper cladding was etched away over a short length (~ 3 mm) for better thermal isolation of the thermometers. The leads ran through Pb tubes to connections higher up on the cryostat.

The thermometer conductances were measured using SHE Corp. model PCB conductance bridges in a four-terminal configuration. With excitation voltages of $10 \mu\text{V}$ below 0.5 K and $100 \mu\text{V}$ above 0.5 K, self-heating was negligible, yet the bridges could provide measuring precisions and accuracies of $\leq 0.5\%$.

Since the SHE bridges were self-balancing, and possessed differential outputs, they could also be used as the sensing device for a temperature controller. A home-built controller,¹² regulated the temperature of the cold resistor T_c , using a heater on the mixing chamber to provide heat input. The temperature resolution of the controller was better than 10^{-4} K.

Overall, about ten thermometers were made using the procedure just described. Four were mounted on the sample limbs shown in Fig. 2 for use in measuring the transverse and longitudinal temperature gradients. These are designated, respectively, as the cold (T_c), hot (T_h), right (T_r), and left (T_l) thermometers. Two others, used for calibrating these four during a measuring run, were thermally connected together via an annealed pure polycrystalline Ag wire. One of these was mounted underneath the sample (in the magnetic field), while the other was mounted on the mixing chamber out of the

field. This latter thermometer (called the reference thermometer—RT) was isolated from the fringing magnetic field at the mixing chamber by placing it inside a NbTi box. Also within this NbTi box was a germanium resistance thermometer (GRT) of known calibration. Since germanium resistance thermometers are sensitive to a magnetic field, GRT was used to calibrate RT at zero magnetic field, and RT was then used to calibrate the other five carbon thermometers against magnetic field.

The crucial thermometers for determining the Righi-Leduc coefficient were T_r and T_l . The temperatures of these thermometers had to be known as accurately as possible, since they were used to measure small temperature differences. They were thus recalibrated *in situ*, in the presence of a given magnetic field, for each measurement as follows.

The magnetic field of interest was established, and the desired heat flow Q_x was sent through the sample. The conductances of T_r and T_l were measured. Q_x was then reduced to zero so that all temperature gradients disappeared, and all of the resistors on the sample were at the temperature of the mixing chamber and its reference thermometer RT. The resistors were all checked against RT in this isothermal situation. Heat was then put into the mixing chamber to raise the first thermometer of interest, say T_r , back to the same conductance reading as it had when the thermal current was flowing through the sample. All of the other resistors, including RT, also increased to this sample temperature. The temperature of T_r was determined using RT. Then a different heat input was used to calibrate the other resistor, T_l , in the same way. This procedure gave an optimal determination of the difference in temperature between T_r and T_l during the original measurement, since they were both calibrated against the same standard in the same way, and in the same magnetic field.

G. The measuring circuit

The electrical circuit for NE and Hall-effect (R_H) measurements is shown in Fig. 4. The standard resistor was used only to check the reference resistor R_r at 4.2 K at the start of each run. At temperatures below 3 K the standard resistor was superconducting and can thus be ignored. A known thermal current (for NE), or electrical current (for R_H), was passed through the sample, and the voltage generated was determined using a SQUID as a null detector. For R_H measurements, where the sample voltage is linearly dependent upon the sample current, a current comparator was used to ramp up two currents simultaneously, one through the sample, and one through R_r , so that the SQUID remained locked. The voltage of interest, V_y , was determined from the ratio of the two currents when the system was balanced. For NE measurements, the voltage of interest varies quadratically with the heater current I_h . Below 1 K, the output voltages were small enough to fit within the dynamic range of the SQUID, and the measuring procedures described just below were used. For NE measurements above 1 K, the voltage of interest was too

large to allow the SQUID to remain locked. In this case, we used a feedback circuit and procedure described elsewhere.⁷

Because the output voltages for NE measurements below 1 K were small, we simply observed the change in SQUID voltage when we applied a known heat input, and then separately calibrated this change by determining the current I_r through R_r that produced the same voltage change. The NE voltage V_y was then $I_r R_r$, where R_r is the resistance. We initially thought that the calibration was essentially independent of the magnetic field B . However, near the end of our studies, we discovered that this was not correct—presumably because of some magnetoresistance in R_r . We therefore made a careful set of calibrations between 1.0 and 2.0 T, where the data had reached the “high-field” limit. A calibration attempt was also made at 2.4 T, but the system was very noisy at such high fields that day, and the calibration data were ambiguous. We therefore concentrate our analysis in this paper upon data up to 2 T, where the behavior of the data is well established.

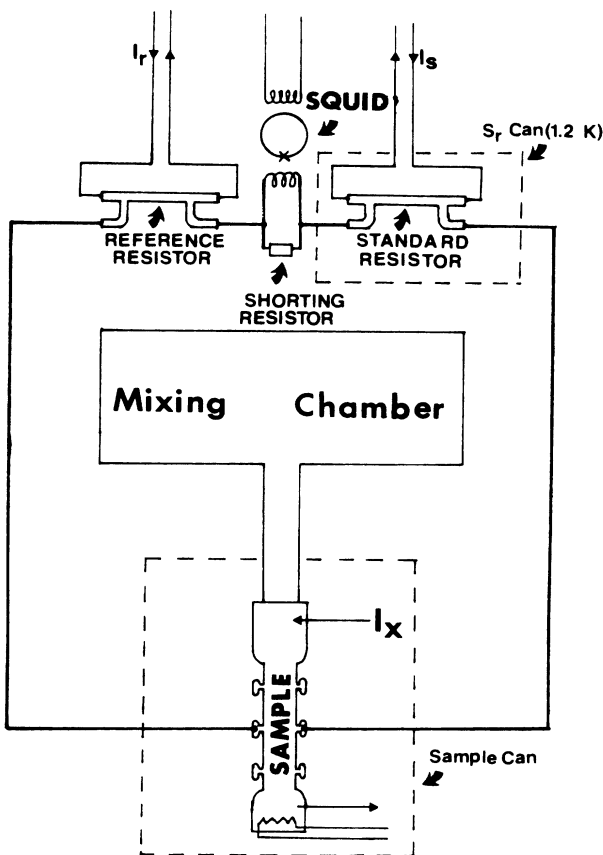


FIG. 4. The basic measuring circuit, containing the sample, the SQUID null detector, a reference resistor for nulling the SQUID, and a PbZn standard resistor used to check resistances accurately at 4.2 K. The standard resistor, which was attached to the 1.2-K helium pot, became superconducting when the 1.2-K pot was pumped down, and thereafter played no role in the measuring circuit.

H. The reference resistor

To get adequate sensitivity in the SQUID circuit, the noise due to the reference resistor must be smaller than the voltage sensitivity needed. To get optimal performance from the current comparator, the reference resistance should have a magnitude close to that of the sample. An ideal reference resistor should have low magnetoresistance, low temperature dependence, low current dependence, low thermopower, and a stable value upon thermal cycling. Our reference resistor was made from Ag wire with 0.4% Pt impurity. Potential leads of the same material were spotwelded onto the body of the resistor wire, so that it was shaped as shown in Fig. 4. At 4.2 K its resistance R_r was $8.78 \times 10^{-6} \Omega$. For a bandwidth of 1 Hz this resistance produces a Johnson noise of 4×10^{-14} V, smaller than the measuring sensitivity we need. R_r could thus be mounted inside the helium bath at 4.2 K, which allowed it to be well away from the magnet. R_r , all the superconducting connections in the SQUID circuit, and the shorting resistor for the SQUID were all shielded from the magnetic field inside the superconducting box. This procedure minimized possible effects of magnetoresistance, temperature dependence, and thermopower of R_r , as well as any noise from vibration of its leads in a magnetic field.

IV. EXPERIMENTAL DATA AND ANALYSIS

As indicated in Eq. (2), the quantities to be measured are the sample thickness t , the transverse voltage V_y , and the total heat flow Q_x through the center of the sample where the voltage measurements are made. Independent checks of t and Q_x can be made from measurements of the Hall and Righi-Leduc coefficients, respectively. We thus discuss measurements of these two quantities before we turn to V_y and NE.

A. The Hall coefficient R_H and sample thickness t

The Hall coefficient R_H is defined as (using $\rho_{yx} = \rho_{xy}$)

$$R_H = \frac{\rho_{yx}}{B} = \frac{E_y}{J_x B} = \frac{V_y/W}{I_x B/Wt} = \frac{V_y t}{I_x B}. \quad (4)$$

For an uncompensated metal, with no open orbits perpendicular to a magnetic field oriented along an axis of at least three-fold symmetry, the high-field limit of R_H is⁵

$$R_H = \frac{1}{(n_e - n_h)ec}, \quad (5)$$

where $n_e - n_h$ is a known quantity for Al.⁵ From Eqs. (4) and (5), we can determine t by measuring I_x , V_y , and B . To determine the sample thickness, the Hall coefficient of aluminum foil taken from the same spool of metal as the sample was measured in a standard helium cryostat at 4.2 K using a SQUID detector in a feedback loop as described elsewhere.⁷ The foil thickness was independently measured using a caliper, and also determined by weighing a piece of measured length and width

and calculating the thickness from the known density of aluminum. The caliper gave a thickness of $(5.1 \pm 0.5) \times 10^{-2}$ mm. Weighing gave $(5.08 \pm 0.10) \times 10^{-2}$ mm. Hall coefficient measurements at 4.2 K gave $(5.05 \pm 0.10) \times 10^{-2}$ mm. As our best estimate we will use the value $t = (5.08 \pm 0.10) \times 10^{-2}$ mm.

Figure 5 shows R_H as a function of B for the sample of interest, as measured in the dilution refrigerator at $T = 0.15$ K. As discussed just above, the sample thickness was assumed to be $(5.08 \pm 0.10) \times 10^{-2}$ mm. Open and filled symbols represent opposite direction of \mathbf{B} . The broken line is the value of $R_H = 1.023 \times 10^{-10} \text{ m}^3 \text{ C}^{-1}$ determined from the known electronic properties of Al [Eq. (5)]. We see that the data reach the high-field limit at about $B = 1.0$ T, and thereafter remain independent of field up to 2.85 T, the highest field used.

B. The Righi-Leduc coefficient and heat flow Q_x

For a sufficiently thick Al sample, all of the heat put into the hot end of the sample would flow to the cold sink through the sample. Q_x would then be simply $Q_x(\text{input})$. For a sample of 0.05 mm thickness, however, some heat may well flow through the much thicker substrate. It was therefore important to independently check that the heat flow through the center of the sample where V_y is measured was approximately as expected. The Righi-Leduc coefficient, R_{RL} , provides a means for measuring this heat flow.

R_{RL} is the thermal analog of R_H . It is defined as

$$R_{RL} = \frac{\Delta T_y / W}{Q_x B} \quad (6)$$

The high-magnetic-field limit of R_{RL} is⁵

$$R_{RL} = -\frac{R_H}{L_0 T} \quad (7)$$

From Eqs. (6) and (7) we see that, since the high-field limit of R_{RL} is a known quantity, we can determine Q_x from measurements of W , ΔT_y , and B . Since ΔT_y was

only 5–10 mK, it was difficult to measure accurately. Under the best conditions, we could resolve ΔT_y only to 5–10%. For convenience, we measured the heat-flow ratio $Q_x(\text{expt})/Q_x(\text{input})$. Here $Q_x(\text{expt})$ is the value inferred from the measured R_{RL} coefficient and Eqs. (6) and (7).

In one of the last runs, when we had established all of our measuring procedures, we measured the heat-flow ratios for an average sample temperature of 0.22 K at -1.6 T, $+2.0$ T twice, and -2.0 T. The values found were 104% at -1.6 T, 90%, and 85% at $+2.0$ T, and 100% at -2.0 T, each with an uncertainty of 5–10%. We see that the negative field values were slightly more positive than the positive field ones. If we linearly average these four values, so as to eliminate effects of field reversal, we find an average of $95 \pm 5\%$. To take account of this probable small heat loss, we multiply our NE data by the factor $1/0.95 = 1.05$, which we take as the “best” R_{RL} correction.

C. The NE coefficient and λ

After a series of measuring runs to check procedures, calibrate thermometers, etc., successful NE coefficient measurements were made in three of four final runs extending over a period of almost two months. We focus here upon data from the last two successful runs—runs 8 and 10, since these data were obtained after we had established and checked our measuring and NE calibration procedures. These data sets were taken with the refrigerator held at 0.147 K and the temperature at the center of the sample raised to about 0.21 K. We also limit our attention to data for B up to about 2.0 T, since only for these data do we have unambiguous NE calibrations. Data at higher fields are described elsewhere.⁷ They were taken before we recognized that the NE calibrations were field dependent. Using the calibration appropriate to $B = 2$ T, they were found to decrease with increasing field to well below the value expected for no enhancement at all. When we later realized that the high-field NE calibrations might be strongly field dependent,

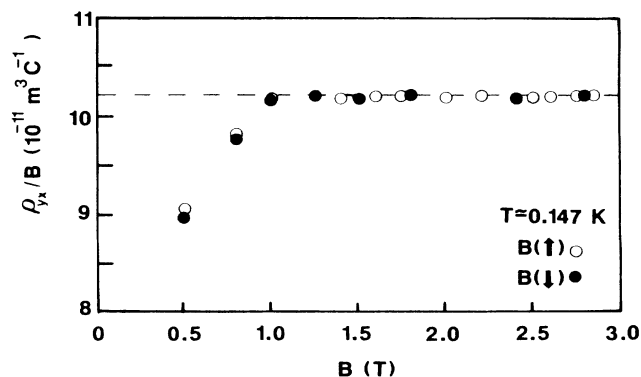


FIG. 5. The Hall coefficient, R_H , of Al at $T = 0.147$ K as a function of magnetic field B . The dashed line is the value predicted from the known electronic structure of Al.

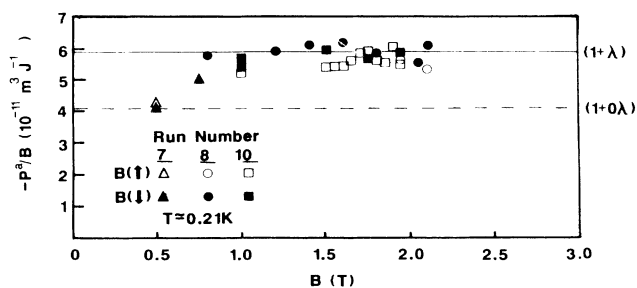


FIG. 6. The Nernst-Ettingshausen coefficient, NE equal to P_a/B , of Al at an average temperature of 0.21 K as a function of magnetic field B . The dashed line labeled $(1+\lambda)$ indicates the value predicted from the electronic specific heat, γ^c , for a simple enhancement of $1+\lambda$. The dashed line labeled $(1+0\lambda)$ is the approximate value expected for no enhancement.

dent, we attempted to determine an appropriate calibration for $B = 2.4$ T, but the system was very noisy, and contradictory results were obtained. We are, thus, not sure whether this apparent decrease is due to an incorrect choice of calibration, or—as proposed in Ref. 7—to the onset of magnetic breakdown.

The symbols in Fig. 6 show the “corrected” NE data from runs 8 and 10 up to $B = 2$ T (along with some low-field points from run 7), obtained by multiplying the raw data by the factor 1.05 to make the R_{RL} correction noted just above. The horizontal solid line in Fig. 6 is the high-field value for NE expected⁵ if $\gamma'/\gamma^c = 1$; i.e., if the NE coefficient is enhanced simply by $(1 + \lambda)$. The horizontal dashed line indicates what would have been expected if γ' were unenhanced. We see that, although the scatter is larger than we would like, the data are consistent with an enhancement of $(1 + \lambda)$ from a magnetic field of 1 T—where they reach the “high-field limit,” up to at least 2 T. Without correction, the data are also roughly consistent with expectation to within experimental uncertainty, but the average falls below the prediction.

V. SUMMARY AND CONCLUSIONS

We have measured the Hall effect (R_H) and the Nernst-Ettingshausen (NE) effect of a thin, polycrystalline Al foil of thickness 0.05 mm at temperatures of 0.15 and 0.22 K, respectively, and in magnetic fields up to 3 T. R_H rises to its high-field limit by 1 T and thereafter remains independent of magnetic field and in agreement with its expected value to within experimental uncertainty of about 1%. The NE coefficient also rises to a constant value at 1 T, which is maintained to about 2 T. Within experimental uncertainty, this value is consistent with expectation for a simple enhancement of $(1 + \lambda)$. NE data above 2 T are not reliable enough to interpret.

ACKNOWLEDGMENTS

The authors thank Professor W. P. Pratt, Jr., Professor P. A. Schroeder, Professor R. D. Spence, and Professor C. L. Foiles, as well as Dr. M. Haerle and Dr. V. Heinen, for helpful suggestions and advice. They also are pleased to acknowledge support for this work from the National Science Foundation through Grant No. DMR-83-03206.

*Current address: Visual Interface Corp., Newberry Park, CA 91320.

¹J. L. Opsal, B. J. Thaler, and J. Bass, *Phys. Rev. Lett.* **36**, 1211 (1976).

²Y. A. Ono and P. L. Taylor, *J. Phys. F* **10**, L129 (1980); *Phys. Rev. B* **22**, 1109 (1980).

³J. W. Wu and G. D. Mahan, *Phys. Rev. B* **30**, 5611 (1984).

⁴J. Rammer and H. Smith, *Rev. Mod. Phys.* **58**, 323 (1986).

⁵B. J. Thaler, R. Fletcher, and J. Bass, *J. Phys. F* **8**, 131 (1978).

⁶R. Fletcher, *Phys. Rev. B* **14**, 4329 (1976).

⁷A. Amjadi, Ph.D. thesis, Michigan State University, 1986 (un-

published).

⁸R. J. Douglas and R. Fletcher, *Philos. Mag.* **32**, 73 (1975).

⁹N. W. Ashcroft and J. W. Wilkins, *Phys. Lett.* **14**, 285 (1965).

¹⁰W. Kesternich and C. Papastaikoudis, *Phys. Status Solidi* **64**, K41 (1974).

¹¹O. V. Lounasmaa, *Experimental Principles and Methods Below 1K* (Academic, New York, 1974).

¹²C.-W. Lee, Ph.D. thesis, Michigan State University, 1980 (unpublished).

¹³H. E. Henrikson, *Rev. Sci. Instrum.* **42**, 1533 (1971).

¹⁴E. I. Dupont Co., Polyimide SP-22.